Oxygen and Proton Pathways in Cytochrome c Oxidase

Ivo Hofacker and Klaus Schulten*
Beckman Institute, University of Illinois at Urbana-Champaign, Urbana, Illinois

ABSTRACT **Cytochrome c oxidase is a redox-driven proton pump, which couples the reduction of oxygen to water to the translocation of protons across the membrane. The recently solved x-ray structures of cytochrome c oxidase permit molecular dynamics simulations of the underlying transport processes. To eventually establish the proton pump mechanism, we investigate the transport of the substrates, oxygen and protons, through the enzyme.**

Molecular dynamics simulations of oxygen diffusion through the protein reveal a well-defined pathway to the oxygen-binding site starting at a hydrophobic cavity near the membrane-exposed surface of subunit I, close to the interface to subunit III.

A large number of water sites are predicted within the protein, which could play an essential role for the transfer of protons in cytochrome c oxidase. The water molecules form two channels along which protons can enter from the cytoplasmic (matrix) side of the protein and reach the binuclear center. A possible pumping mechanism is proposed that involves a shuttling motion of a glutamic acid side chain, which could then transfer a proton to a propionate group of heme α_3. Proteins 30:100–107, 1998. © 1998 Wiley-Liss, Inc.

INTRODUCTION

Cytochrome c oxidase (CcO) is the terminal enzyme of the respiratory chain in eukaryotes and most bacteria. It is located in the inner membrane of mitochondria and the cell membrane of prokaryotes, where it reduces molecular oxygen to water and, coupled to the redox reaction, pumps protons across the membrane.[1,2] Recently, two crystal structures of CcO, one from the soil bacterium *Paracoccus denitrificans,*[3] the other from bovine heart,[4,5] have been published. Although knowledge of the static structure is not sufficient to understand the molecular mechanism that couples oxygen reduction to proton translocation, it provides the prerequisite for theoretical and computational studies aimed at elucidating the underlying mechanism.

CcO contains a varying number of subunits, three of which (I, II, and III) are conserved across species,

as well as two copper centers and two heme groups (see Fig. 1). Cu_A is a bimetallic Cu-Cu center found in subunit II and serves as the primary acceptor for electrons from cytochrome c. Subunit I contains the six-coordinate, low-spin heme a and a binuclear center consisting of the five-coordinate, high-spin heme a_3 and Cu_B, which forms the catalytic site for oxygen reduction. Electron transfer is believed to proceed from Cu_A via heme a to the binuclear center.

In this work we study the pathways for transport of oxygen and protons by predicting the distribution of water molecules in the protein and by molecular dynamics (MD) simulation of oxygen diffusion as well as key proton transfer steps. We suggest a possible mechanism of proton pumping that emerged from the results. The fact that structures from two very different organisms are available is particularly helpful in this respect because any plausible mechanism should be feasible in both enzymes.

We will use residue numbering for *P. denitrificans* throughout this paper unless noted otherwise.

METHODS

Coordinates for the bovine structure were taken from the pdb databank entry pdb1occ.ent, and the *P. denitrificans* structure was provided by H. Michel. All MD simulations reported were performed by using the program X-PLOR[7] with the CHARMm22 all hydrogen force field.[8] Hydrogens were added to the structures by using X-PLOR's hbuild function. The forcefield contains parameters for a heme group with six-coordinated Fe(II). Bond and angle equilibrium values for the five-coordinated iron in heme a_3 as well as the copper ligands were taken from the x-ray structure.[3] Missing force constants for bonds and angles involving copper were set to 65 kcal/mol $Å^2$ for bonds (same as heme Fe-His bond) and 30 kcal/rad^2 for angles (same as heme-His Fe-NE2-CE1).

The charge distribution for Cu_B and its three histidine ligands in the CU(I) state were obtained from a fit of the electrostatic potential generated by an ab initio wavefunction for a model ion, yielding a
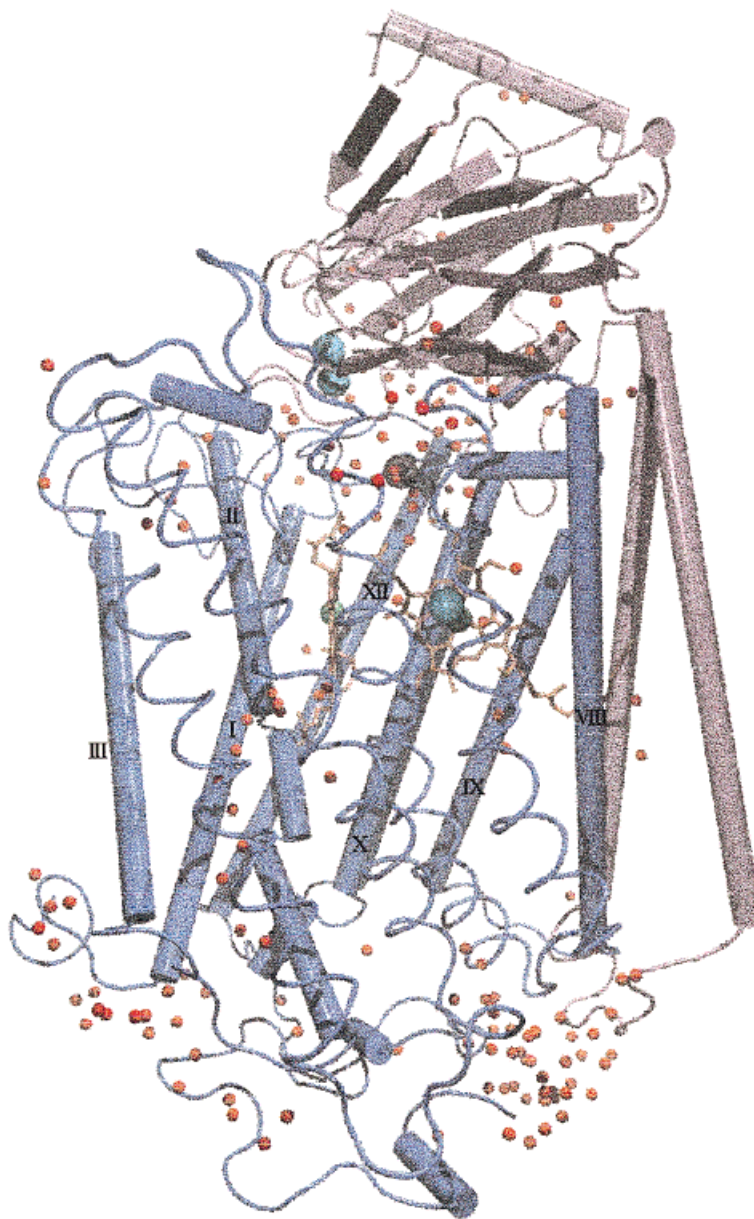
Fig. 1. Distribution of water molecules placed in the structure of *Paracoccus denitrificans.* Water oxygens are shown as small red spheres, large spheres are metals, Cu is presented in cyan, heme-Fe in green, and Mg in silver; subunits I and II are shown in blue and mauve. α-Helices are rendered as cylinders, except for SU-I helices IV–VII, which are rendered as coils to admit a better view into the structure; roman numerals denote helix numbering in SU-I. All figures were produced by VMD[6] and povray.

partial charge of 0.383 for the copper (Todd Martinez, personal communication). The model ion was comprised of Cu surrounded by three imidazole rings in the geometry specified by the crystal structure reported in Ref. 3 with an overall singly positive charge. The program PSGVB[9] was used to calculate the electronic charge distribution, with an effective potential to describe the inner electrons of Cu[10] and basis sets of double-zeta quality.[11] The detailed charge distribution around Cu_A was not calculated because it is less relevant for the work presented here. Instead, atomic partial charges were estimated as follows: a partial charge of 0.75 was used for the copper atoms, the two histidine ligands were given a charge of $+0.25$, and the two deprotonated cysteine ligands a total charge of -0.5 each.

The simulations involved only subunits I and II, which together consist of approximately 13,000 atoms and were performed in vacuo. To avoid deformation of the structure because of the missing subunits, membrane, and bulk water, C_a positions were restrained to the x-ray coordinates by using a harmonic potential with a force constant of 1 kcal/Å^2. Electrostatic interactions were cut off at 14 Å by using a switching function starting at 12 Å.

Water molecules buried in the protein were predicted by using the DOWSER* program of Jan Hermans and coworkers.[12] DOWSER places water molecules by searching for hydrophilic cavities, where

*Available at http://femto.med.unc.edu/Research/Dowser.html

hydrophilicity is measured as the interaction energy between a water molecule in the cavity and the surrounding protein. Cavities with an interaction energy of less than -12 kcal/mol are filled with water molecules and are left empty otherwise. Recent NMR experiments[13] have shown, however, that large enough hydrophobic cavities can contain disordered water molecules. Such water molecules would not be predicted by DOWSER, but one can safely assume that they would amount only to a very small fraction of internal water molecules in CcO. In the case of the subunits I, II, such cavities do not arise in close proximity to the binuclear center, but arise distant from this center; the possible error will be discussed below.

Two parameters of the DOWSER program were changed slightly compared with the program as distributed. The minimum distance between water oxygens was increased from 2.0 to 2.2 Å, to avoid overly close packing of water molecules; because DOWSER will test only possible water sites buried in the protein, the probe radius used for deciding whether a position is buried or on the surface was changed from 0.8 to 1.4 Å.

The water molecules placed by DOWSER were then refined through 500 steps of minimization in X-PLOR with all protein atoms except hydrogens fixed. After minimization, interaction energies for each water molecule were once more computed by X-PLOR and water molecules with $E > -12$ kcal/ mol, if any, were deleted. This removed excess water molecules in rare cases where DOWSER would place two water molecules too close in a small cavity. Finally, the system was equilibrated to a temperature of 300K through 50 ps of MD simulation during which the water molecules could rearrange further. This refinement of water positions predicted by DOWSER is particularly important for larger cavities because DOWSER neglects interactions between water molecules. The water molecules within the proton pathways described below typically moved less than 2 Å during the equilibration process.

Oxygen diffusion simulations used the locally enhanced sampling (LES) technique of Elber and coworkers.[14,15] The technique is based on a time-dependent Hartree approximation and admits the inclusion of several copies of the oxygen molecule in a single MD simulation with the following three modifications: different copies of the oxygen do not interact with each other; the interaction between oxygen and protein is scaled down by the number of copies; the mass of the oxygen molecules is reduced by the same factor, which restores the normal equations of motion for the oxygen. This speeds up the simulations in two ways: (1) several oxygen trajectories can be obtained in a single MD run, which improves statistics; (2) the diffusion itself is speeded up as a consequence of the reduced energy barriers for movement of the oxygen molecules and due to

their greater speed resulting from the reduced mass. For our simulations, 20 copies of molecular oxygen proved sufficient to achieve the desired speedup.

RESULTS AND DISCUSSION
Oxygen Pathways

The question, along which paths oxygen reaches its binding site at the binuclear center, has received little attention so far. On the basis of their crystal structure, Tsukihara et al.[5] proposed three possible pathways:

- a "shortest path" leading from Phe 237 and Trp 288 to the Cu_B ligand His 291 (*P. denitrificans* F273, W323, and H326);
- following the hydroxyfarnesylethyl group of heme a_3 to the binuclear center with its entrance between the two transmembrane helices of SU II;
- through a channel of loosely packed aromatic residues, starting at the V-shaped cleft formed by SU III.

Independently, based on the *P. denitrificans* data, the latter pathway has been recently tested by Riistama et al.[16] who found that mutation of Val 279 to Ile raises the $K_{M,app}$ for O_2 by a factor of 10–15. Unfortunately, Val 279 is too close to the binding site to reliably distinguish between obstruction of the pathway and effects on the local binding kinetics.

We studied the diffusion of oxygen for both structures in molecular dynamics simulations by using the locally enhanced sampling (LES) method, which uses several oxygen molecules in a single simulation (see Methods). In a first set of simulations, the oxygen molecules were placed at the approximate binding site between Cu_B and the heme a_3 iron. The simulations favored the "third" pathway suggested in Ref. 5, which then was tested further in simulations with the initial oxygen position close to the entrance of this path. Four of the simulations are described below.

At the start of the first simulation of the *P. denitrificans* structure, 20 oxygen molecules were placed at the binding site. Oxygen molecules were observed to move roughly along the third pathway; within only 50 ps, 18 of the 20 oxygen molecules had moved to a large cavity some 15 Å away from the binuclear center as shown in Figure 2. The cavity is very hydrophobic and was therefore left empty by DOWSER. A narrow channel, lined with hydrophobic aromatic residues, connects the cavity to the binuclear center. The narrowest point of the passage lies between the conserved residues Phe 274 and Trp 164.

Diffusion toward the binuclear center along this path was tested in a second simulation with the initial oxygen position on the surface of subunit I close to His 187. After 50 ps, one oxygen had moved into the protein and the cavity mentioned before. At
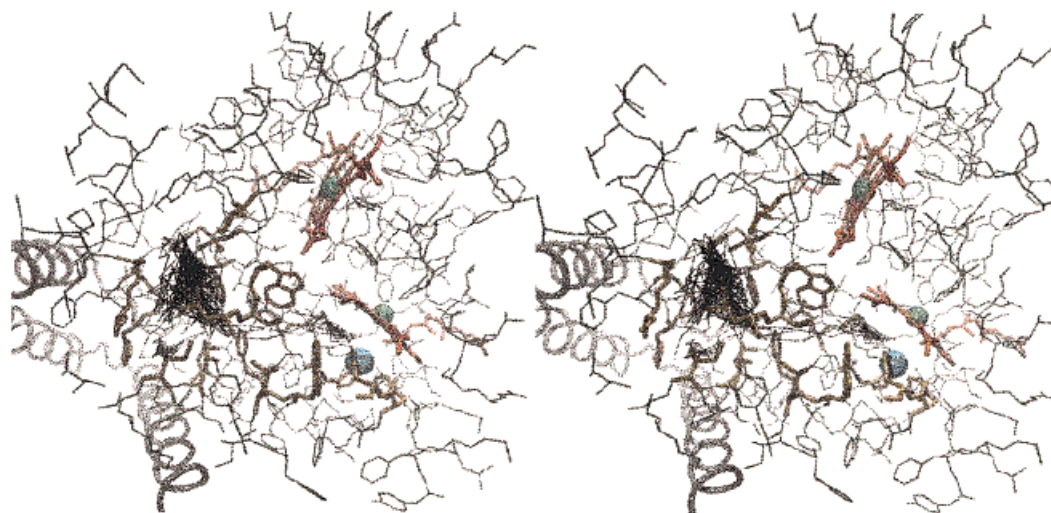
Fig. 2.   Stereo view of the trajectory of an oxygen molecule diffusing in the *P. denitrificans* structure (black line) seen from the periplasmic side of the protein. Hemes are shown in red, and residues lining the trajectory in ochre. The gray spirals on the left represent helices of subunit III (not part of the simulation). The thick tangle of lines on the left marks a cavity where the oxygens spend most of the time.

this point, the simulation was restarted with all 20 oxygen molecules in the cavity and during the next 50 ps 5 of the 20 oxygen molecules reached the binuclear center. The trajectory for one of these oxygen molecules can be seen in Figures 2 and 3.

A trajectory for the bovine structure is shown in Figure 3 (bottom). Although the narrow part of the channel is very similar to that in the *P. denitrificans* structure, the cavity on the left is split up into several smaller ones. In this simulation, oxygen molecules were initially placed close to the start of the narrow channel and within 50 ps, 4 of 20 oxygen molecules came close to the binuclear center, whereas 14 eventually escaped from the protein. Note also that the trajectory shown in Figure 3 does not extend all the way to the binuclear center; this shortcoming is due to a water molecule that is bound to Cu_B and blocks the path. A corresponding water molecule in the *P. denitrificans* structure was found to move out of the way, permitting access to the binding site; the respective water molecule in the bovine structure has slightly less free space in this region and, hence, is less mobile. On the actual millisecond timescale for oxygen binding, this immobility of the water molecule is not likely to be an impediment, but it causes an insurmountable obstacle on the picosecond timescale of our simulation (as explained in Methods, the LES approximation speeds up the dynamics of the oxygen, but not of the rest of the system).

In a fourth simulation, 10 oxygen molecules were placed at the binuclear center of the bovine structure with the above mentioned water molecule removed. With only 10 copies, the diffusion proceeds much more slowly, but all oxygen molecules moved in the direction of the above pathway, and 3 reached the large cavity within 100 ps.

Small changes in the protein conformation have a strong influence on the time needed for oxygen molecules to diffuse to or from the binuclear center, and our method is therefore not suitable for an estimate of the diffusion rate of oxygen to the binuclear center. However, the space explored by the oxygen molecules on their path to the binuclear center was very similar in all simulations and essentially restricted to the volume covered by the trajectories shown in Figures 2 and 3. Furthermore, the trajectories were very similar for both structures. Taken together, the simulations provide good evidence that oxygen molecules reach the binuclear center via a particular pathway starting close to the interface to subunit III.

Proton Channels

Proton transfer in proteins can occur either through protonatable residues with multiple conformations or through chains of hydrogen bonds. The latter often involve water molecules, which can form efficient proton wires. Neither of the CcO structures presently available resolves bound water molecules. We attempted, therefore, to establish likely positions of bound water molecules using for this purpose the program DOWSER and MD simulations (see Methods).

Our calculations predict approximately 130 water molecules within subunits I and II of each structure. The distribution of water molecules for the *P. denitrificans* structure can be seen in Figure 1 and is very similar for the bovine structure. A large number of water molecules are predicted in the interface of subunits I and II and near the propionate groups of the hemes, permitting proton exchange with the bulk solvent on the periplasmic side (intermembrane space). Furthermore, the water molecules so placed
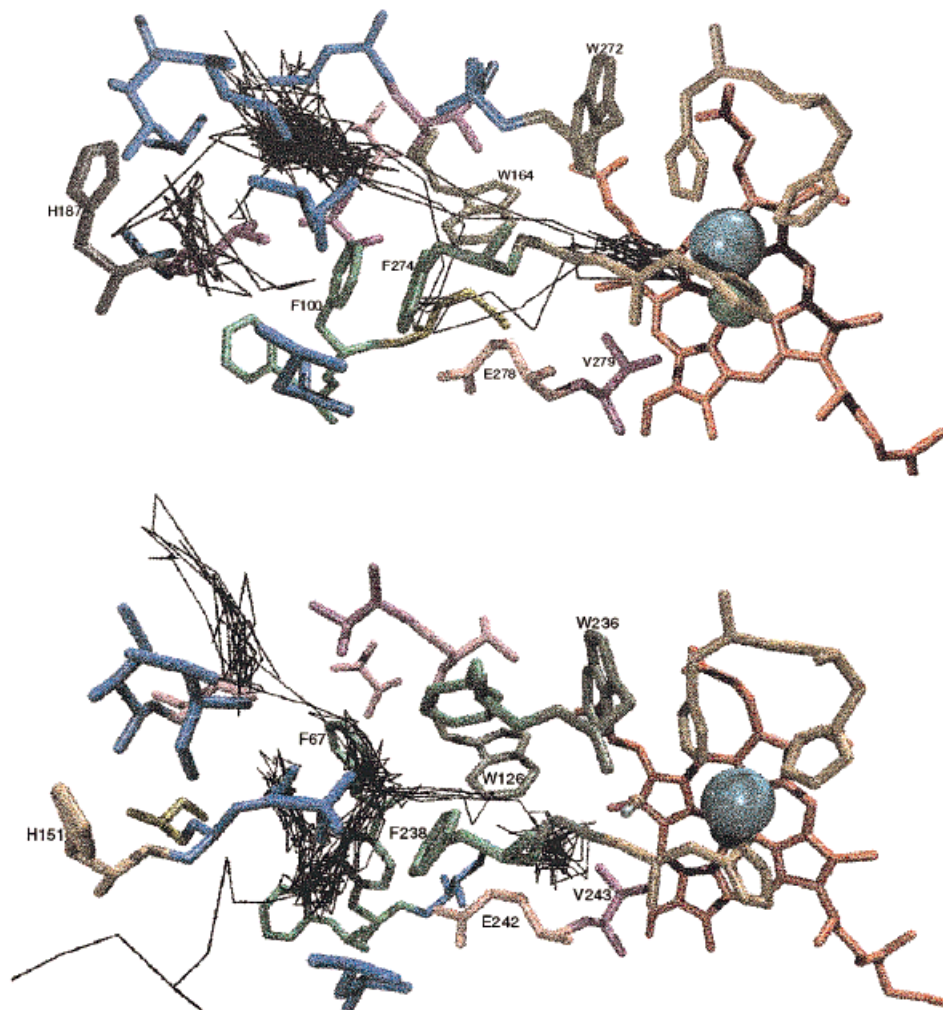
Fig. 3. Oxygen trajectories for the *P. denitrificans* (top) and bovine structure (bottom) viewed approximately parallel to the membrane plane. For the bovine structure the trajectory of two oxygens is shown; one escaped from the protein on the lower left, and the other moved toward the binding site until blocked by a water molecule. Color coding: Phe, Trp green; Leu blue; Val pink; His ochre; Met yellow; Heme red; and copper cyan.

exhibit two possible channels for taking up protons from the cytoplasmic (matrix) side of CcO (see Fig. 4).

One channel is formed by a chain of water molecules leading from Asp 124 on the inside of the membrane to Glu 278. Although this channel has already been identified[3] on the basis of the x-ray structure and known mutant data, it is interesting to note that the hydrogen bond chain shown in Figure 4 is formed almost exclusively by the water molecules placed in this study. The polar residues lining the channel seem to serve only to stabilize the water molecules. This provides a rationale for the observation in Ref. 17 that mutation of polar residues along the channel reduces the enzyme's efficiency only slightly. The acidic residues Glu 278 and Asp 124, on the other hand, are essential for enzyme function.[18–20] Because mutation of Asp 124 affects proton pumping, but not redox activity, this pathway was proposed to transport protons to be pumped.[20,21] Glu 278 as shown in Fig. 4 is unprotonated; once protonated the side group forms a hydrogen bond to the backbone oxygen of Met 99 while the hydrogen bonds to water molecules are weakened or broken.

Another possible proton channel described in Ref. 3 leads from Ser 291, which is in contact with external water molecules, via Lys 354 to Tyr 280. As shown in Figure 4, two water molecules were placed within this channel, which could contribute to the transport of protons consumed in the reduction of oxygen. In the x-ray structure Lys 354 is close to Ser 291 and most likely unprotonated. The channel, consequently, exhibits a gap between Lys 354 and Thr 351 which is not bridged by water molecules. Our MD simulations of the *P. denitrificans* structure revealed that Lys 354 is flexible enough to bridge the gap by movement of its C_β—N_ϵ chain. Once proto-
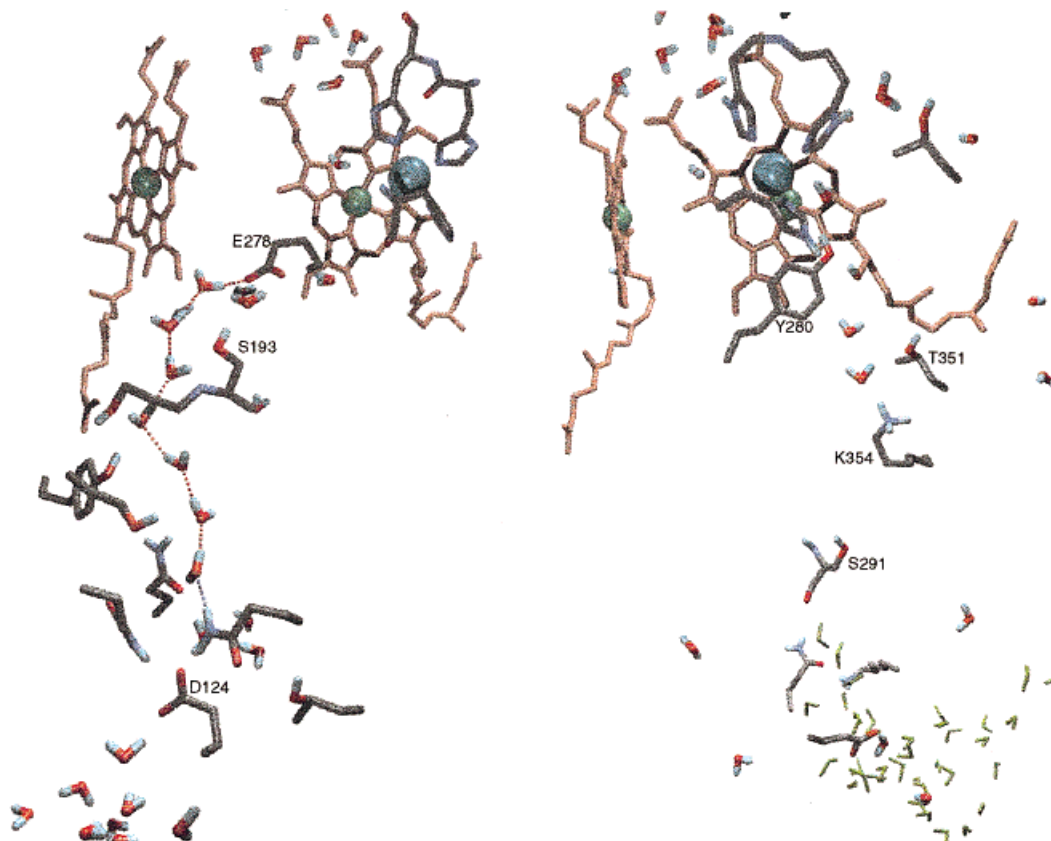
Fig. 4.   Two channels suitable for proton transfer. Left: A chain of hydrogen bonds (broken lines) involving seven water molecules connects Asp 124 to Glu 278. Right: Protons could be transfered from Lys 354 to the binuclear center via two waters, the heme hydroxyl group and Tyr 280. The lysine is flexible and has swung upwards from its original position close to Ser 291, bridging the gap to Thr 351. An open cavity connects Ser 291 (S291) to bulk water on the inside of the membrane. Water molecules filling this cavity are shown in green to distinguish them from buried waters placed by DOWSER. The two views are rotated by approximately 36° relative to each other.

nated, the lysine head group moved within 50 ps by 3.1 Å to a position close to Thr 351, as shown in fig. 4. The water molecule shown just above the lysine was originally placed between the lysine and Ser 291, but moved upwards following the lysine head group. In case of the bovine structure, the lysine stays closer to the serine.

For the bovine enzyme Tsukihara et al.[5] proposed a variant of the first pathway that continues from Ser 157 (*P. denitrificans* Ser 193) upward along Ser 149, Ser 108, Thr 146, and Ser 115 instead of leading to the glutamic acid. In addition, the authors proposed a third pathway between helices XI and XII involving a hydroxyl group of heme a. Neither of these is supported by our placement of water molecules. Although the water positions suggested in Figure 10 of Ref. 5 are reproduced, both paths contain too few water molecules to bridge the gaps between polar residues, nor do they contain flexible protonatable residues.

Although the placement of water molecules identifies an efficient pathway for protons up to Glu 278, there is no obvious continuation of the pathway from there. One possibility is that the protonated glutamic acid side chain could flip upward and deliver its proton either to the binuclear center or to a heme a_3 propionate group as originally proposed in Ref. 3. The large number of water molecules placed just above this propionate group makes it a prime candidate for the acceptor of pumped protons. Within the short time span accessible to MD simulations, such a conformational change of Glu 278 could not be observed. However, it can be induced easily by pulling the side chain upward.

Our water placement predicts one (bovine) or two (*P. denitrificans*) water molecules in the vicinity of Cu_B, one of them binding to Cu_B, as suggested by recent EXAFS data.[22] Once oxygen binds, these water molecules could become available to stabilize Glu 278 in the flipped position through hydrogen bonding and help transfer its proton.

We have modeled this scenario in an MD simulation of the *P. denitrificans* structure starting with the glutamic acid side chain in the upward conformation. The configuration after 100 ps is shown in Figure 5. The two water molecules originally close to
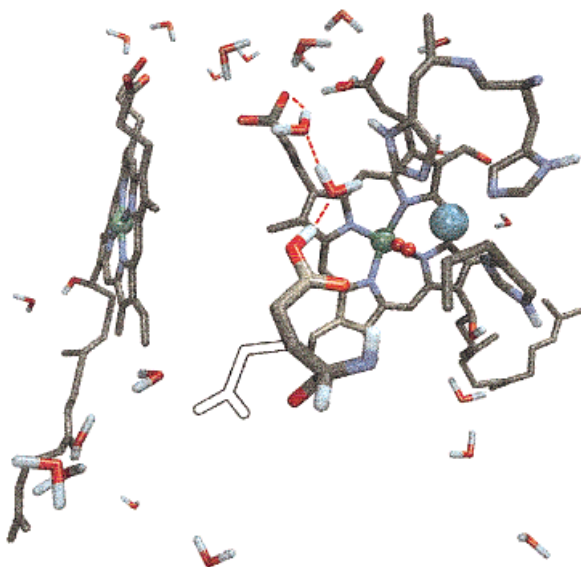
Fig. 5. Flipped side chain conformation for Glu 278. After rotating into a cavity between helix VI and the heme group, the protonated glutamic acid can transfer its proton along the broken red line to the heme a$_3$ propionate group. The black outline shows the configuration of Glu 278 in the structure reported in Ref. 3.
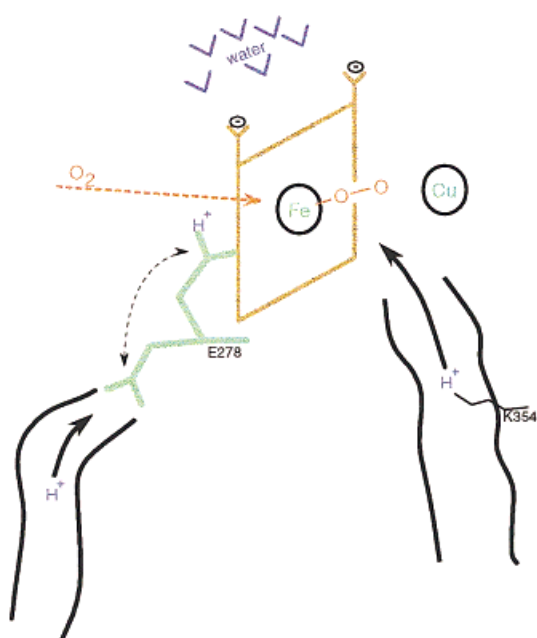

Fig. 6. Possible mechanism for proton pumping: By flipping the side chain of Glu 278, a proton comes close to the Heme propionate group. When a proton is delivered to the binuclear center via the other proton channel, Glu 278 deprotonates, transfers the proton to the propionate group, and flips back into its original conformation. The red dotted arrow indicates the direction from which oxygen diffuses to the binuclear center.

the copper have rearranged themselves to form a hydrogen bond chain to one of the heme propionate groups. As suggested in Fig. 6, the proton on the glutamic acid could now be pumped to the propionate

group while transfer to the oxygen is hindered by the positive charge on Cu$_B$. Uptake of a consumed proton along the other channel could cause the glutamic acid to deprotonate and provide the free energy necessary for the pumping. Compared with the "histidine shuttle" mechanism described in Ref. 3, 23, 24, shuttling of Glu 278 does not require breaking of chemical bonds; however, Glu 278 cannot transfer two protons in one step.

Recently, Konstantinov et. al.[25] showed that CcO can react with H$_2$O$_2$ even when the lysine channel is blocked by mutation of Lys 354, implying that Glu 278 should be able to supply chemical protons to the binuclear center as well. Because both the propionate and the bound oxygen at the binuclear center are approximately 6 Å away from the flipped Glu 278, it seems likely that its proton would be transferred to the oxygen once the propionate is protonated.

CONCLUSIONS

Identifying the pathways along which the oxygen and proton substrates travel within CcO is a crucial step toward understanding the proton pump mechanism of CcO. The results of our simulations indicate that oxygen molecules diffuse toward the binding site at the binuclear center along a well-defined path. The existence of such a channel could be important for controlling access and trapping of oxygen at the binuclear center. In the case of the bovine structure, a water molecule presented an obstacle for the path of the oxygen to the binuclear center on the time scale of 50 ps, whereas such water moved out of the way in the case of the *P. denitrificans* structure. Test simulations revealed that this water, in the case of both the *P. denitrificans* and bovine structure becomes immobile for a reduced, i.e., CU(II), state of the binuclear center. One may conclude that the water adopts a gatekeeper function at the oxygen entrance to the binuclear center.

The diffusing oxygen molecules show a preference for hydrophobic cavities, a large and a small cavity in the case of the *P. denitrificans* structure and three small cavities in the case of the bovine structure. These cavities did not receive water molecules from DOWSER; the large cavity possibly might contain disordered water, not placed by DOWSER, in which case the oxygen would avoid the cavity.

By predicting sites of water molecules buried in the protein, we are able to pinpoint proton transfer pathways with higher accuracy and confidence than by inspection of the structure alone. The results indicate two pathways for proton uptake from the inside of the membrane in good agreement with results from site-directed mutagenesis experiments. Particularly striking is the chain of water molecules leading up to Glu 278 and the large number of water molecules connecting the heme a$_3$ propionate groups to the other side of the membrane. We, therefore,

suggest a transfer path for pumped protons via Glu 278 and the propionate group, with Glu 278 forming the "switch" between the proton input and output states of the enzyme.

REFERENCES

1. Calhoun, M.W., Thomas, J.W., Gennis, R.B. The cytochrome oxidase superfamily of redox-driven proton pumps. Trends Biochem. Sci. 19:325, 1994.
2. Malatesta, F., Antonioni, G., Sarti, P., Brunori, M. Structure and function of a molecular machine: Cytochrome c oxidase. Biophys. Chem. 54:1–33, 1995.
3. Iwata, S., Ostermeier, C., Ludwig, B., Michel, H. Structure at 2.8 Å resolution of cytochrome c oxidase from *Paracoccus denitrificans.* Nature, 376:660–669, 1995.
4. Tsukihara, T., Aoyama, H., Yamashita, E., Tomizaki, T., Yamaguchi, H., Shinnzawha-Itoh, K., Nakashima, R., Yaono, R., Yoshikawa, S. Structures of metal sites of oxidized bovine heart cytochrome c oxidase at 2.8 Å. Science 269:1069–1074, 1995.
5. Tsukihara, T., Aoyama, H., Yamashita, E., Tomizaki, T., Yamaguchi, H., Shinnzawha-Itoh, K., Nakashima, R., Yaono, R., Yoshikawa, S. The whole structure of the 13-subunit oxidized cytochrome c oxidase at 2.8 Å. Science 272:1136–1144, 1996.
6. Humphrey, William F., Dalke, Andrew, Schulten, Klaus. VMD—Visual molecular dynamics. J. Mol. Graphics 14:33–38, 1996.
7. Brünger, Axel T. "X-PLOR, Version 3.1: A System for X-ray Crystallography and NMR." Yale University: The Howard Hughes Medical Institute and Department of Molecular Biophysics and Biochemistry, 1992.
8. MacKerell, A.D., Jr., Karplus, M. All-hydrogen empirical potential for molecular modeling and dynamics studies of proteins using the CHARMM22 force field. 1996. Manuscript in preparation.
9. Ringnalda, Murco N., Langlois, Jean-Marc, Greeley, Burnham H., Russo, Thomas V., Muller, Richard P., Marten, Bryan, Won, Youngdo, Jr., Donnelly, Robert E., Pollard, W. Thomas, Miller, Gregory H., Goddard, William A. III, and Friesner, Richard A. PS-GVB v0.08. Schroedinger Inc., 1993.
10. Hay, P.J., Wadt, W.R. Ab initio effective core potentials for molecular calculations. Potentials for the transition metal atoms Sc to Hg. J. Chem. Phys. 82:270–283, 1984.
11. Hehre, J., Ditchfield, R., Pople, J.A. Self-consistent molecular orbital methods XII. Further extensions of Gaussian-type basis sets for use in molecular orbital studies of organic molecules. J. Chem. Phys. 56:2257–2261, 1972.
12. Zhang, Li, Hermans, Jan. Hydrophilicity of cavities in proteins. Proteins Struct. Func. Genet. 24:433–438, 1996.
13. Ernst, J.A., Clubb, R.T., Zhou, H.X., Gronenborn, A.M., Clore, G.M. Demonstration of positionally disordered water within a protein hydrophobic cavity by NMR. Science 267:1813–1817, 1995.
14. Elber, R., Karplus, M. Enhanced sampling in molecular dynamics: Use of the time-dependent Hartree approximation for a simulation of carbon monoxide diffusion through myoglobin. J. Am. Chem. Soc. 112:9161–9175, 1990.
15. Roitberg, A., Elber, R. Modelling side chains in peptides and proteins: Application of the locally enhanced sampling technique and the simulated annealing methods to find minimum energy conformations. J. Chem. Phys. 95:9277–9287, 1991.
16. Riistama, S., Puustinen, A., García-Horsman, A., Iwata, S., Michel, H., Wikström, M. Channelling of dioxygen into the respiratory enzyme. Biochim. Biophys. Acta 1275:1–4, 1996.
17. Mitchell, David M., Fetter, John R., Gennis, Robert B., Site-directed mutagenesis of residues lining a putative proton transfer pathway in cytochrome c oxidase from *rhodobacter sphaeroides.* Biochemistry 35:13089, 1996.
18. Hosler, J.P., Ferguson-Miller, S., Calhoun, M.W., Thomas, J.W., Hill, J., Lemieux, L., Ma, J., Georgiou, C., Fetter, J., Shapleigh, J.P., et al. Insight into the active-site structure and function of cytochrome oxidase by analysis of site-directed mutants of bacterial cytochrome aa_3 and cytochrome bo. J. Bioenerg. Biomembr. 25:1210–136, 1993.
19. Fetter, J.R., Qian, J., Shapleigh, J., Thomas, J.W., García-Horsman, A., Schmidt, E., Hosler, J., Babcock, G.T., Gennis, R.B., Ferguson-Miller, S. Possible proton relay pathways in cytochrome c oxidase. Proc. Natl. Acad. Sci. USA 92:1604–1608, 1995.
20. García-Horsman, J.A., Puustinen, A., Gennis, R.B., Wikström, M. Proton transfer in cytochrome bo_3 ubiquinol oxidase of *E. coli:* Second-site mutations in subunit I that restore proton pumping in the mutant Asp135→ASN. Biochemistry 34:4428–4433, 1995.
21. Thomas, J.W., Puustinen, A., Alben, K.O., Gennis, R.B., Wikström, M. Substitution of asparagine for aspartate-135 in subunit i of the cytochrome bo ubiquinol oxidase of escherichia coli eliminates proton-pumping activity. Biochemistry 32:10923–10928, 1993.
22. Fann, Y.C., Ahmed, I., Blackburn, N.J., Boswell, J.S., Verkhovskaya, M.L., Hoffman, B.M., Wikström, M. Structure of Cu-B in the binuclear heme-copper center of the cytochrome aa(3)-type quinol oxidase from bacillus subtilis—an ENDOR and EXAFS study. Biochemistry 34:10245–10255, 1995.
23. Morgan, J.E., Verkhovsky, M.I., Wikström, M. The histidine cycle—a new model for proton translocation in the respiratory heme-copper oxidases. J. Bioenerg. Biomembr. 26:599–608, 1994.
24. Wikström, M., Bogachev, A., Finel, M., Morgan, J.E., Puustinen, A., Raitio, M., Verkhovskaya, M., Verkhovsky, M.I. Mechanism of proton translocation by the respiratory oxidases—the histidine cycle. Biochim. Biophys. Acta Bioenerg. 1187:106–111, 1994.
25. Konstantinov, A.A., Siletsky, S., Mitchell, D., Kaulen, Andrey, Gennis, R.B. The roles of the two proton input channels in cytochrome c oxidase from *rhodobacter sphaeroides* probed by the effects of site-directed mutations on time-resolved electrogenic intraprotein proton transfer. Proc. Natl. Acad. Sci. USA 1997 94:9085–9090, 1997.